



In situ structural characterization of picene thin films by X-ray scattering: Vacuum versus O₂ atmosphere

T. Hosokai^{a,*}, A. Hinderhofer^b, A. Vorobiev^c, C. Lorch^b, T. Watanabe^a, T. Koganezawa^d, A. Gerlach^b, N. Yoshimoto^a, Y. Kubozono^e, F. Schreiber^b

^a Department of Materials and Science, Iwate University, Ueda 4-3-5, Morioka, Iwate 0208551, Japan

^b Institut für Angewandte Physik, Universität Tübingen, Auf der Morgenstelle 10, Tübingen 72076, Germany

^c ESRF, 6 Rue Jules Horowitz, Boîte Postale 220, 38043 Grenoble Cedex 9, France

^d Japan Synchrotron Radiation Research Institute, 1-1-1 Kouto, Sayo-cho, Hyogo 6795198, Japan

^e Research Laboratory for Surface Science, Okayama University, Okayama 7008530, Japan

ARTICLE INFO

Article history:

Received 29 March 2012

In final form 3 July 2012

Available online 10 July 2012

ABSTRACT

Structure and morphology of picene films under vacuum and O₂ atmosphere were studied by *in situ* synchrotron X-ray scattering. We observed that picene films exhibit a highly oriented and ordered structure, which is similar to the one reported for picene single crystals. Furthermore, we found that the film structure determined under vacuum remains nearly unchanged under O₂ atmosphere. The results provide new insights into a high hole mobility and O₂ gas sensing mechanism previously reported for picene thin film-based organic field-effect transistors.

© 2012 Elsevier B.V. All rights reserved.

1. Introduction

Recently, the interest in the organic semiconductor picene (Figure 1a) has rapidly increased due to reports on its excellent charge transport properties and O₂ gas sensing ability in organic field-effect transistors (OFETs) [1,2]. A remarkable OFET hole mobility of 5 cm² V⁻¹ s⁻¹ was observed for picene FETs under O₂ atmosphere, whereas the mobility was lower by more than two orders of magnitude in vacuum. This change of device performance was shown to be reversible upon repeated cycles of O₂ exposure and evacuation, promising potential use of picene FETs as O₂ gas sensors [3–5]. To study this effect several investigations were conducted, for example, to find an upper limit of the gas sensitivity and to improve the performance by modifying the device structure [4,5]. In addition, fundamental studies on the mechanism of the mobility enhancement of picene FETs were carried out [3,6]. Kawasaki et al. adopted a multiple shallow trap and release model to explain the change in device performance by O₂ gas exposure [3]. They found that mobility increases are not due to the increase of the charge carrier density, i.e. not due to chemical doping of the films, but based on the reduction of shallow trap states existing at the interface between picene and the gate insulator or in the bulk film. The reduction of trap states by O₂ gas exposure was also confirmed by temperature dependent measurements of the device performance [6].

* Corresponding author. Fax: +81 19 621 6351.

E-mail address: thosokai@iwate-u.ac.jp (T. Hosokai).

To obtain information on the trap states and the interaction mechanism, photoemission spectroscopy has been applied. Wang et al. reported in a valence-band photoemission study that a pristine multilayer film of picene deposited on Ag (110) exhibits gap states originating from structural defects in the film [7]. Furthermore, they proposed a strong interaction between picene and O₂ resulting in a change of the electronic structure of picene. Such a strong interaction between both compounds is in agreement with X-ray photoemission spectra which show the irreversible binding of O₂ to picene deposited on an Au/Stainless steel substrate, with a 1:1 mol ratio even under ultrahigh vacuum (UHV) conditions ($p = 10^{-6}$ Pa) [4].

However, these photoemission studies cannot explain the reversibility of device performance of picene FETs under O₂ exposure/evacuation. In general, the effects of gas exposure on organic films can be very diverse. For example, there are reports that a chemical interaction between organic molecules and gas molecules can change the crystallinity, film thickness and roughness of a thin film [8–10]. It was further reported that even for weak interaction with inert gas molecules, gap states can be induced in organic films due to structural defects/imperfections [11]. Therefore, to understand the O₂ gas sensing mechanism of picene FETs, the effect of O₂ gas exposure on the picene thin film structure should be also investigated.

Here, we performed *in situ* synchrotron based X-ray reflectivity (XRR), grazing incidence X-ray diffraction (GIXD) and rocking scans, on picene/SiO₂ under UHV and under O₂ atmosphere. The *in situ* characterization using synchrotron radiation, provides detailed structural information, such as in-plane and out-of-plane

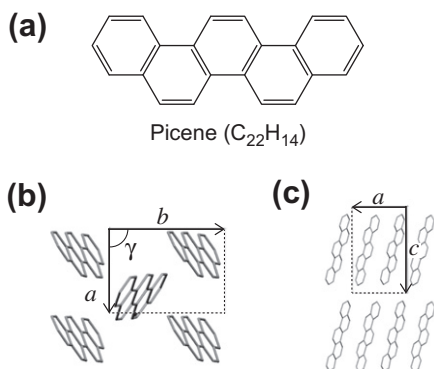


Figure 1. (a) Chemical structure of picene and its crystal structure projected from *c*-axis (b) and *b*-axis (c) reported in Ref. [12]. The unit cell contains two molecules.

lattice constants, (coherent) film thickness, surface roughness and mosaicity of crystallites in the films. After comparing the picene thin film structure with the already known single crystal structure [12], we discuss in detail the structural influences of O₂ exposure on picene thin films.

2. Experimental procedure

All experiments presented here were performed at beamline ID10B [13] at the ESRF in Grenoble (France), using a home-built portable UHV chamber [14] at a wavelength of 0.925 Å. The experiments were partly reproduced at beamline 19B2 at the SPring-8 in Harima (Japan). Picene (purity: 99.9 %) was purchased from NARD Co Ltd. and was used without further purification. As substrates we used Si (100) wafers covered with native oxide. Before film growth, the substrates were cleaned ultrasonically with acetone, isopropanol and ultrapure water, followed by heating to 700 K in the UHV growth chamber (base pressure: $\sim 10^{-8}$ Pa). Thin films of picene were fabricated by organic molecular beam deposition [15,16] at a substrate temperature of 303 K. The deposition rate was set to ~ 0.4 nm/min monitored by a water-cooled quartz crystal microbalance calibrated by XRR. After deposition *in situ* XRR, GIXD and rocking scans were conducted. For all scattering geometries a scintillation counter (Cyberstar) was used as detector. The resolution in q_z and q_{xy} was defined with a pair of horizontal and vertical slits on the detector arm as well as by the shape of the incoming beam (defined by all optical elements upstream of the sample). In particular the resolution was $\Delta q_z = 0.002 \text{ \AA}^{-1}$ for XRR, $\Delta q_{xy} = 0.021 \text{ \AA}^{-1}$ for GIXD, and $\sim 0.002^\circ$ for rocking scans limited by the width of the (111) reflection of the first (diamond) monochromator with its heat-induced partial deformation and internal strain. The angle of incidence and the detector angle relative to the sample surface for GIXD was 0.10° . The film thickness (δ) and the root-mean-squared surface roughness (σ) of the picene film, which were determined by fitting the XRR data with the MOTOFIT software applying the Parratt formalism [17], are given in Table 1. Ultrapure O₂ gas (Air products Inc., 5 N) was dosed into the UHV

Table 1

Fitted values of film thickness δ , surface roughness σ and FWHM of rocking curve of picene thin films under various conditions: as-deposited in UHV (i), under O₂ atmosphere (500 torr) (ii), and in UHV after O₂ exposure (iii).

| | δ (nm) | σ (nm) | Rocking FWHM ($^\circ$) |
|-------|------------------|------------------|------------------------------|
| (i) | 35.6 ± 1.0 | 3.6 ± 0.1 | 0.0069 ± 0.0003 |
| (ii) | 36.9 ± 1.0 | 3.7 ± 0.1 | 0.0067 ± 0.0003 |
| (iii) | 37.0 ± 1.0 | 3.7 ± 0.1 | 0.0067 ± 0.0003 |

chamber via a leak valve up to a pressure of nearly 500 torr. These conditions are comparable to those under which picene FETs showed a hole mobility of $5 \text{ cm}^2 \text{ V}^{-1} \text{ s}^{-1}$ [3]. The stainless-steel gas supply line between the O₂ gas cylinder and the leak valve was evacuated with a membrane pump before use. Data measured under O₂ atmosphere are compared to data gathered prior to O₂ exposure and to data measured after returning to vacuum conditions (10^{-5} Pa) to check for possible damage caused by simultaneous exposure to X-ray radiation and O₂. During the experiment the film was irradiated by the X-ray beam for four hours in total.

3. Results and discussion

3.1. In situ characterization of picene thin film

Figure 2a–c shows XRR and GIXD data from a picene thin film grown on SiO₂. The measurements were performed first in vacuum after growth (i), then under O₂ atmosphere (500 torr) (ii), and finally in vacuum again (iii). For better comparison in Figure 2c, we subtracted the background originating from scattering at O₂ gas from the GIXD data (ii), which is marked as (ii)′.

The XRR data (i) in Figure 2a show four prominent Bragg reflections at $q_z = (0.465 \pm 0.001) \text{ \AA}^{-1} \cdot n$ with $n = 1, 2, 3, 4$ and two smaller reflections at $q_z = 1.16$ and 1.63 \AA^{-1} , respectively. The q_z -value of the former reflections correspond to a lattice constant of $d = 2\pi/q_z \equiv (13.51 \pm 0.03) \text{ \AA}$ which is nearly identical to that observed in single crystals for the *c*-axis (13.515 Å) (see Figure 1c) in Ref. [12]. Hence, these Bragg reflections are attributed to a standing-up orientation of picene molecules on SiO₂, as was found in Ref. [4]. The two smaller reflections marked by (∇), with corresponding lattice spacings $d = 5.42$ and 3.85 \AA , are not explained by the bulk powder diffraction data [12], suggesting the formation of a small amount of domains with another structure and probably lying down or tilted molecular orientation. The periodicity of the Laue oscillations Δq_{Laue} around the (001)-reflection shown in Figure 2b corresponds to a coherent out-of-plane film thickness δ_{coherent} with $\Delta q_{\text{Laue}} = 2\pi/\delta_{\text{coherent}} = 2\pi/Nd$ (N being the number of coherent layers with d). For the pristine picene thin film (i) δ_{coherent} is calculated to be $(34 \pm 2) \text{ nm}$, which is comparable to the film thickness δ ($=35.6 \text{ nm}$), indicating that picene molecules in the standing-up orientation form coherently ordered films.

The GIXD data (i) in Figure 2c show clear diffraction peaks at $q_{xy} = 1.01, 1.26, 1.51, 1.57, 1.82, 1.87$ and 2.01 \AA^{-1} , respectively. We note that the two peaks marked by (\star) at 1.57 and 1.87 \AA^{-1} cannot be assigned to reflections from the single crystal phase. These reflections may also stem from a second polymorph similar to the additional reflections in Figure 2a. Since picene grows as in-plane powder, we can simulate the diffraction pattern (i) using the following equation [18]:

$$q_{xy} = \frac{2\pi}{ab \cdot \sin \gamma} \sqrt{(hb)^2 + (ka)^2 - 2hkba \cdot \cos \gamma}. \quad (1)$$

Neglecting the two peaks marked with (\star) and using a least-square fitting routine we obtain in-plane unit cell parameters of $a = 8.33(0) \text{ \AA}$, $b = 6.22(9) \text{ \AA}$ and $\gamma = 90.27(7)^\circ$. Those values are only slightly different from those of the single crystal structure, i.e. $a = 8.480 \text{ \AA}$, $b = 6.154 \text{ \AA}$ and $\gamma = 90.46^\circ$ [12], and from the single crystal surface found by low-energy electron diffraction, i.e. $a = 8.6 \text{ \AA}$, $b = 6.3 \text{ \AA}$ and $\gamma = 90^\circ$ [19]. This agreement suggests that the electronic structure of crystalline domains in picene thin films should be similar to what was found for corresponding single crystals, i.e. a highest-occupied molecular orbital band-dispersion of several hundreds meV along both the *a*- and the *b*-axis as predicted theoretically in Ref. [20] and observed experimentally in Ref. [19].

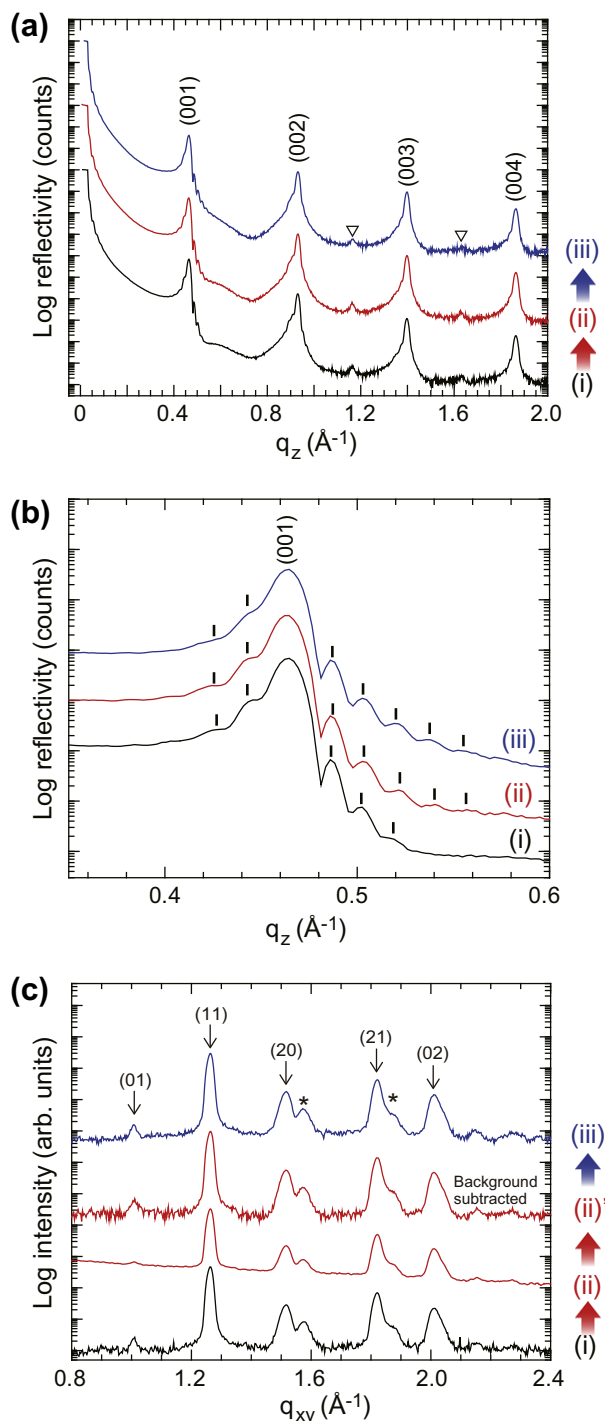


Figure 2. XRR (a) and GIXD (c) of a picene thin film on a SiO₂/Si wafer under different measurement conditions; as-deposited in UHV (i), under O₂ atmosphere (500 torr)(ii), in UHV after O₂ exposure (iii). For better comparability in (ii)' the background was subtracted by using polynomial functions. Indexing for GIXD was done by theoretical simulation based on monoclinic structure in Ref. [12]. (b) Expanded XRR around the first Bragg reflection (001). The solid bars depict the peaks of the Laue oscillation. The ∇ in (a) and \star in (c) are the reflections from unknown structures.

Figure 3a shows a rocking scan at the (001) Bragg peak of the picene films in vacuum and under O₂ atmosphere. The mosaicity of the picene crystallites is estimated by the full width at half maximum (FWHM) of the rocking curve, which is highly relevant for the charge carrier mobility of organic semiconductors [21]. By fitting the data (i) with GAUSSIAN functions as shown in Figure 4b, a

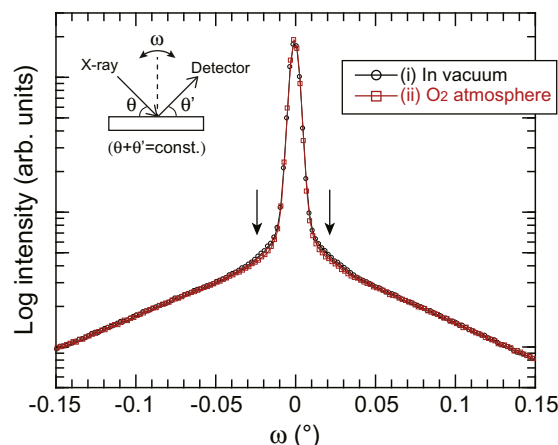


Figure 3. Normalized rocking curves at the (001) Bragg reflection of the picene thin film in UHV (circle) and under O₂ atmosphere (square). The inset is a schematic of the measurement geometry. The arrows indicate the suppression of tailing intensity of the rocking peak in (ii).

FWHM of only $(0.0069 \pm 0.0003)^\circ$ is obtained. The value is clearly smaller than that reported for other organic semiconductor materials with good charge transport, such as diindenoperylene, pentacene, perfluoropentacene and perfluorinated copper phthalocyanine thin films [22–24]. Thus, we may conclude that one reason for the high hole mobility in picene FETs – even without O₂ gas exposure [3] – is the remarkable crystalline order of the picene thin films.

3.2. Influence of O₂ gas exposure

Here, we compare X-ray data from a picene thin film under UHV (i and iii) and under oxygen exposure (ii) (Figure 2). The fit results for the XRR and rocking curves are shown in Figure 4a–b, with the relevant parameters summarized in Table 1. The analysis shows clearly that O₂ exposure causes only a very small irreversible change in film morphology. In Figure 2a and c all Bragg reflections both in the out-of-plane and in-plane direction are within the error bars identical. Hence, it is concluded that the O₂ gas exposure does not significantly influence the unit cell structure of picene. This is in strong contrast to the intercalation of alkali-metal atoms (K or Rb) into picene thin films, where it is theoretically predicted that a 1:1 mol ratio can result in a clear change in the unit cell structure of picene [1]. The film thickness and roughness increase by only 1%, and the rocking width decreases very slightly after the O₂ exposure. These changes are derived from thickness oscillations in Figure 4a and from the suppression of the peak tailing (depicted by arrows) in Figure 3. The small gas exposure-induced change is also seen in the Laue pattern in Figure 2b, where the higher order oscillations become slightly more pronounced. However, the most important result here is that these changes are not reversible under O₂ evacuation. This phenomenon is inconsistent with the reversible O₂ gas sensing properties of picene FETs. Therefore, we conclude that the O₂ gas exposure induces a small change in film morphology, however, this change is not related to the reversible device properties of picene FETs.

In the case of titanium (or ruthenium) phthalocyanine films, other gas sensing organic materials, an increase in both, film thickness and roughness, of ~5–10% by NO_x gas exposure was observed. This was explained by the penetration of the gas molecules through the surface to the bulk of the films or just a rearrangement of the surface structure [9,10]. However, the change in film thickness and roughness for picene thin films is much smaller than in those cases. Thus, we speculate that the interaction between O₂

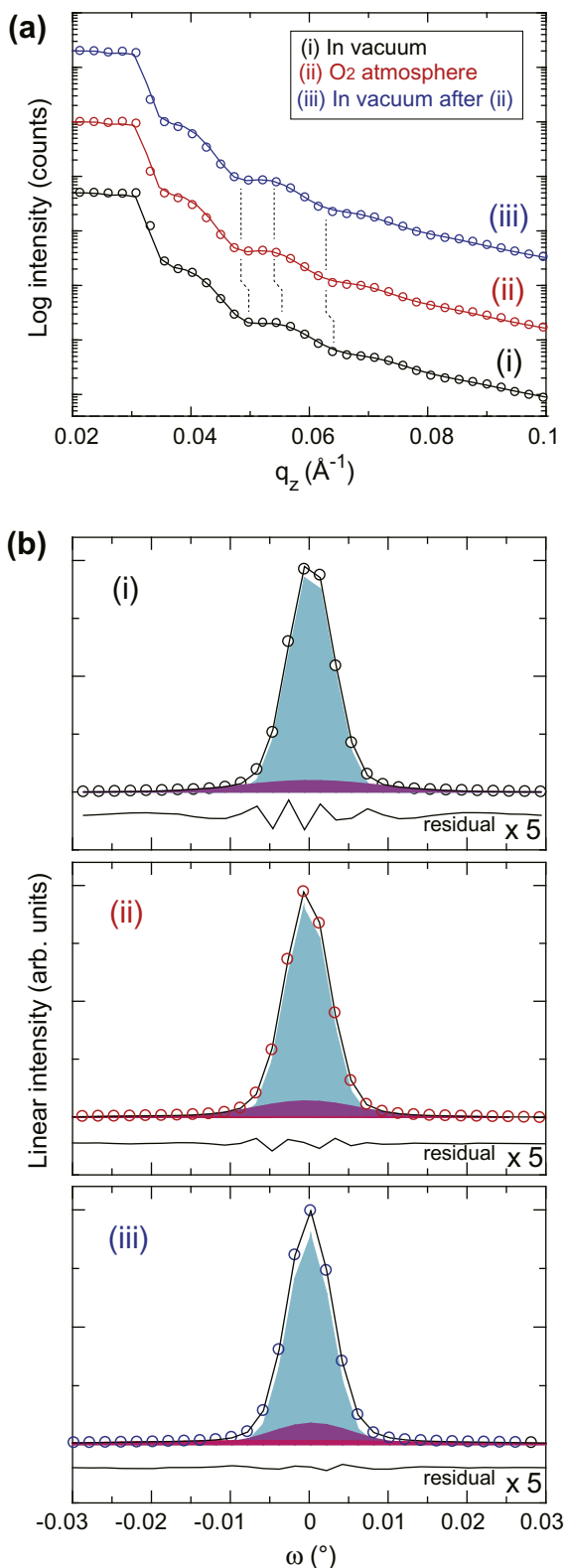


Figure 4. Fitting results for XRR at low q_z region (a) and for the rocking curves (b). Empty circles and solid lines display experimental results and theoretical fitting results, respectively. Broken lines in (a) indicates the shift of dips and peaks of the Kiessig oscillations. For the fitting in (b) GAUSSIAN functions were used.

gas and picene is fundamentally different compared to the interaction of gas molecules with the above-mentioned phthalocyanines. Specifically, our results imply that picene thin films are structurally

very inert to O_2 gas exposure. This consideration is contradictory to the reports by Wang et al. in Ref. [7] and Kaji et al. in Ref. [4], which are showing strong interactions between picene thin films and O_2 gas, but is consistent to Xin et al., where a clean surface of a picene single crystal without special cleaning process was obtained under UHV conditions [19]. The different results in Refs. [7,4] may be connected to the much thinner film thickness or to the different substrates used for their experiments.

3.3. Stability of picene thin films to X-ray exposure

Organic thin films may degrade under long-term exposure of high intensity, highly focused X-ray radiation [25]. However, for picene thin films good agreement of XRR and GIXD data, measured in UHV before and after O_2 exposure was observed (see (i) and (iii) in Figure 2a–c). This result demonstrates the stability of picene against simultaneous exposure to X-ray irradiation and O_2 , similar to the chemical stability reported in Ref. [1]. This is different from similar compounds like pentacene and rubrene, which exhibit more pronounced photo oxidation [8,26]. This stability of picene may be beneficial for applications in organic devices.

4. Conclusion

In order to obtain information on the mechanism of reversible mobility change of picene FETs under O_2 gas exposure/evacuation, we studied the film structure of picene under two different conditions, in vacuum and under O_2 atmosphere. Picene thin films were found to be strongly oriented and of excellent structural order, indicating excellent transport properties in picene FETs as demonstrated before [1–3]. After O_2 gas exposure, we found only very small and irreversible changes in film morphology. Therefore, we conclude that the O_2 related enhanced hole mobility in picene FETs is not caused by a structural reorganization induced by O_2 gas exposure.

Acknowledgments

The authors thank I. Hiroswa (JASRI/SPring-8) and F. Bussolotti (Chiba University) for helpful discussions and the ESRF for experimental support. This work was financially supported partly by the DFG, the Alexander von Humboldt Foundation and Grant-in-Aid for Scientific Research, JSPS (1560005). The synchrotron radiation experiments at the BL19B2 of SPring-8 were performed with the approval of the Japan Synchrotron Radiation Research Institute (JASRI) (Proposal Nos. 2011AB0036 and 2011A1843).

References

- [1] Y. Kubozono et al., *Phys. Chem. Chem. Phys.* 13 (2011) 16476.
- [2] H. Okamoto, N. Kawasaki, Y. Kaji, Y. Kubozono, A. Fujiwara, M. Yamaji, *J. Am. Chem. Soc.* 130 (2008) 10470.
- [3] N. Kawasaki, Y. Kubozono, H. Okamoto, A. Fujiwara, M. Yamaji, *Appl. Phys. Lett.* 94 (2009) 043310.
- [4] Y. Kaji et al., *Appl. Phys. Lett.* 95 (2009) 183302.
- [5] X. Lee et al., *Org. Electr.* 11 (2010) 1394.
- [6] C. Voz, A. Marsal, C. Moreno, J. Puigdollers, R. Alcobilla, *Synth. Met.* 161 (2012) 2554.
- [7] Y. Wang, S.D. Motta, F. Negri, R. Friedlein, *J. Am. Chem. Soc.* 133 (2011) 10054.
- [8] H. Yang et al., *J. Phys. Chem. C* 112 (2008) 16161.
- [9] V.R. Albertini et al., *Appl. Phys. Lett.* 82 (2003) 3868.
- [10] A. Generosi et al., *Appl. Phys. Lett.* 87 (2005) 181904.
- [11] T. Sueyoshi, H. Kakuta, M. Ono, K. Sakamoto, S. Kera, N. Ueno, *Appl. Phys. Lett.* 96 (2010) 093303.
- [12] A. De, R. Ghosh, S. Roychowdhury, P. Roychowdhury, *Acta Cryst. C* 41 (1985) 907.
- [13] D.-M. Smilgies, N. Boudet, B. Struth, O. Konovalov, *J. Synchrotron Rad.* 12 (2005) 329.
- [14] T. Hosokai, A. Gerlach, A. Hinderhofer, C. Frank, G. Ligorio, U. Heinemeyer, A. Vorobiev, F. Schreiber, *Appl. Phys. Lett.* 97 (2010) 063301.
- [15] G. Witte, C. Wöll, *J. Mater. Res.* 19 (2004) 1889.

- [16] F. Schreiber, *Phys. Stat. Sol.* 201 (2004) 1037.
- [17] A. Nelson, *J. Appl. Crystallogr.* 39 (2006) 273.
- [18] S. Schiefer, M. Huth, A. Dobrinevski, B. Nickel, *J. Am. Chem. Soc.* 129 (2007) 10316.
- [19] Q. Xin et al., *Phys. Rev. Lett.* 108 (2012) 226401.
- [20] T. Kosugi, T. Miyake, S. Ishibashi, R. Arita, H. Aoki, *J. Phys. Soc. Jpn.* 78 (2009) 113704.
- [21] N. Karl, Charge carrier mobility in organic crystals, in: R. Farchioni, G. Grosso (Eds.), *Organic Electronics Materials*, Springer, Berlin, 2001, p. 283.
- [22] A.C. Dürr, F. Schreiber, M. Münch, N. Karl, B. Krause, V. Kruppa, H. Dosch, *Appl. Phys. Lett.* 81 (2002) 2276.
- [23] A. Hinderhofer et al., *J. Chem. Phys.* 127 (2007) 194705.
- [24] J.O. Ossó, F. Schreiber, V. Kruppa, H. Dosch, M. Garriga, M.I. Alonso, F. Cerdeira, *Adv. Funct. Mater.* 12 (2002) 455.
- [25] A. Neuhold et al., *Nucl. Instrum. Methods B* 284 (2012) 64.
- [26] M. Kytka, A. Gerlach, J. Kováč, F. Schreiber, *Appl. Phys. Lett.* 90 (2007) 131911.